

Neutron Storage in a Longitudinally Vibrating Silicon Crystal

R. HOCK,^{a*} K. D. LISS,^b A. MAGERL,^c O. G. RANDL^c AND A. REMHOF^d

^aMineralogisches Institut, Universität Würzburg, Am Hubland, D-97074 Würzburg, Germany, ^bEuropean Synchrotron Radiation Facility, BP 220, F-38043 Grenoble CEDEX, France, ^cInstitut Max von Laue–Paul Langevin, BP 156, F-38042 Grenoble CEDEX, France, and ^dPhysikalisches Institut, Ruhr-Universität Bochum, D-44780 Bochum, Germany. E-mail: r.hock@rzbox.uni-wuerzburg.de

(Received 30 May 1997; accepted 3 September 1997)

Abstract

The time structure and integrated diffraction profile of cold neutrons of wavelength $\lambda = 6.27 \text{ \AA}$ transmitted through a longitudinally vibrating silicon crystal were calculated by Monte Carlo simulations and measured on the backscattering spectrometer IN10 at the Institut Laue–Langevin. Neutrons of velocity $v_N = 630 \text{ ms}^{-1}$ require $t_T = 158.5 \text{ \mu s}$ for direct transit through the 100 mm-long silicon resonator. This time is long compared with the vibration period $T_p = 22.3 \text{ \mu s}$ and most of the neutrons experience multiple Bragg reflections in the oscillating Doppler-strain field. Monte Carlo calculations predict that neutrons will be stored in the crystal and released with a time structure determined by the vibration period and by the energy width of the incident beam. For a continuous beam, the usual time modulation of the diffracted neutrons with twice the vibration frequency is expected. If a neutron pulse much shorter than the vibration period impinges on the crystal, the transmitted signal should be a decaying sequence of pulses separated by the vibration period. For pulses which are long compared with the vibration period, the effect of neutron storage should be manifest as a delayed staircase-like intensity variation on both pulse edges. A silicon crystal was set with the (111) lattice planes in backreflection and excited in a $\lambda/2$ resonance at 44.78 kHz. A typical deformation amplitude was $u_0 = 1 \text{ \mu m}$ corresponding to a scattering range of $\Delta E = \pm 1.9 \text{ \mu eV}$. The response of the $\lambda/2$ resonator to a quasicontinuous beam and to neutron pulses of lengths $\Delta t_p = 3 \text{ ms}$ and 33 \mu s FWHM was measured. Experiments were performed with neutron beams of two energy widths $\Delta E = \pm 0.35$ and $\pm 1.23 \text{ \mu eV}$. In agreement with the Monte Carlo simulations, neutron storage in the silicon crystal was observed. The storage time was 250 \mu s for both long and short incident pulses. This time equals about 11 vibration periods of the crystal resonator and is in good agreement with the calculations for the Si 111 reflection and chosen vibration parameters. A first indication of the dependence of the time structure on the energy width of the neutron beam was seen in the experiments. The predicted pulsed structure of the transmitted signal

in response to neutron pulses shorter than the vibration period could not be resolved. With a shortest incident pulse width of $\Delta t_p = 33 \text{ \mu s}$, the condition $\Delta t_p \ll T_p$ was not fulfilled. The measured transmission profile is in good agreement with the calculations for the $\lambda/2$ resonator. Compared with vibrating crystals excited into higher harmonics at the same applied strain, the $\lambda/2$ resonator has a lower reflectivity.

1. Introduction

A standing sound wave with a frequency f_s in the kilohertz to megahertz range and typical amplitudes u_0 of a few micrometres to a few hundred \AA introduces a dynamic gradient in the lattice spacing of an initially perfect crystal. If a pure longitudinal mode is excited, this gradient is one dimensional in the direction of the sound wavevector \mathbf{k}_s . From an incident polychromatic neutron beam, the vibrating crystal diffracts an enlarged wavelength band compared with the non-vibrating perfect crystal. Both the Doppler effect and lattice strain contribute to this enhanced wavelength acceptance (Michalec *et al.*, 1971; Buras *et al.*, 1972). The integrated diffracted intensity depends linearly on the amplitude of the sound wave, if the sound wavelength λ_s greatly exceeds the extinction length Λ . Thus, vibrating crystals have been attracting interest as intensity-to-resolution tunable monochromators for neutrons (Iolin *et al.*, 1996; Michalec *et al.*, 1988; Kulda *et al.*, 1988; Stoica & Popovici, 1984) and other applications in neutron scattering instrumentation such as fast neutron choppers (Kulda *et al.*, 1981; Mikula *et al.*, 1976). Since the gradient in the interplanar spacing is time dependent, the diffracted beam itself is time modulated. If the transit time t_T of the neutrons through the crystal is short compared with half a vibration period $T_p/2$, single scattering dominates the diffraction process and the neutron beam is modulated with twice the sound frequency. Most experiments on the diffraction of neutrons on vibrating crystals have been performed under the condition $t_T \leq T_p/2$.

If the flight time of the neutrons through the crystal is much longer than half a vibration period $t_T \gg T_p/2$,

multiple scattering of neutrons occurs. For scattering at Bragg angles $\Theta < 90^\circ$ the diffracted intensity is then reduced compared with the intensity diffracted from the same lattice planes under the condition $t_T \ll T_p/2$. The intensity reduction can be explained by sound-induced secondary extinction (Mikula *et al.*, 1974). For the use of a vibrating crystal as a monochromator, this reduced reflectivity is unfavourable. No decrease in reflectivity due to sound-induced secondary extinction effects is observed in backscattering experiments on vibrating crystals excited into standing-wave modes if the crystal thickness exceeds $5/2\lambda_s$. Silicon crystals vibrating at megahertz frequencies with sound wave amplitudes up to 250 Å set in backscattering geometry with their (111) lattice planes have a high neutron reflectivity (Hock *et al.*, 1993). At constant dynamic strain, the reflectivity does not change over a wide range of vibration frequencies and amplitudes, even though multiple-scattering events increase quickly with increasing sound frequency. Monte Carlo calculations reproduce quantitatively the measured transmission curves and explain, on a microscopic basis, why the high reflectivity of vibrating crystals persists in backscattering geometry into the multiple-scattering regime (Hock & Kulda, 1994).

Multiple scattering of neutrons in backscattering geometry can be used for the storage of cold neutrons. Recently, a storage device based on multiple reflections of neutrons between two perfect (111)-oriented crystal plates cut from a monolithic silicon crystal was proposed (Schuster *et al.*, 1990) and built (Schuster *et al.*, 1991; Jericha *et al.*, 1996). Multiple reflections on $hkl|-h-k-l$ reflection pairs inside a longitudinally vibrating silicon crystal set up in a fully asymmetric diffraction geometry can be used to generate neutron pulses as short as 1.3 μs (Mikula *et al.*, 1980; Kulda *et al.*, 1981).

The need for both further investigation of the potential of vibrating crystals as intensity-to-resolution tunable monochromators in backscattering diffraction devices and the experimental verification of neutron storage in the oscillating Doppler-strain field stimulated this work. Transmission curves of the 111 reflection were recorded with the crystal vibrating in resonance and are in agreement with calculations for the $\lambda/2$ resonator. Measurements of the time structure of the transmitted neutron beam were performed with incident neutron pulses much longer than and comparable with the vibration period. The experiments were repeated with incident neutron beams of two different energy widths. In all experiments the time structure of the transmitted beam was measured for three settings of the sample crystal: (a) with the silicon crystal rotated out of the backreflection condition, (b) with the sample set in backreflection, but without excitation of the resonance vibrations, and (c) with the silicon crystal set in backreflection and excited into resonance vibrations.

With the first setting, the time width and shape of the neutron pulses produced by the chopper were measured. The pulses are then affected only by absorption in the silicon sample. The second experiment measured the neutron pulse shape transmitted through the nonvibrating crystal in backreflection position. In the last experiment the time structure of the neutron beam transmitted through the vibrating crystal was finally recorded.

In the following section we give details of the backscattering experiments on the neutron spectrometer IN10. In §§3 and 4 the experimental results and predictions of Monte Carlo simulations are presented. In the last two sections, §§5 and 6, points of agreement and disagreement between the experimental findings and the simulations are discussed. Conclusions are drawn concerning modified and optimized experiments for future investigation of neutron storage in vibrating crystals.

2. Experimental methods

From a Czochralski-grown silicon single-crystal cylinder of 30 mm diameter a bar of 100 mm length was cut. The long sample axis corresponded to the [111] direction. Plane parallel flats of 20 mm height were cut normal to the direction $[-110]$. The crystal faces were then mechanically polished. Disc-shaped piezoceramic transducers of 25 mm diameter and 1 mm thickness were glued onto the flats in the middle of the silicon crystal bar. The piezoceramic has a high mechanical coupling factor $k_p = 0.62$ and a low mechanical Q value of 120. With a frequency constant of $N_p = 2100$, the transducers have a planar eigen resonance at $f_p = 84$ kHz.

To excite the resonance vibrations, a sinusoidal voltage was applied by a radio-frequency generator to one of the ceramic transducers. The second transducer was used as a detector to monitor the silicon-crystal resonances. The frequency generator supplied a maximum output voltage of 1 V and could be tuned to a precision of $\Delta f = 0.1$ Hz. The generator signal was then amplified by a wide-band radio-frequency amplifier with 50 W power and a maximum gain factor of 50 dB. The $\lambda/2$ resonance of the silicon sample was found at $f_s = 44.78$ kHz. From this frequency and the sound wavelength of 0.2 m, a sound velocity $v_{[111]} = 8956$ ms^{-1} in the [111] direction was calculated.

The silicon-crystal-transducer composite was mounted on a goniometer head and placed at the sample position of the backscattering spectrometer IN10. The crystal was aligned with the scattering vector $\tau_{[111]}$ parallel to the incident beam. The backscattering spectrometer was operated in the high-resolution mode with a polished Si 111 monochromator mounted on the Doppler drive.

2.1. *Vibration-amplitude dependence of the transmission curves*

Transmission curves of the vibrating crystal as a function of sound amplitude were measured with a ^3He detector placed 1 cm behind the sample. The monochromator Doppler drive was set to 6 Hz. At this frequency the Si 111 monochromator of IN10 reflects a neutron beam with an energy range $\Delta E = \pm 7.4 \mu\text{eV}$ centred at $E_0 = 2080 \mu\text{eV}$. The centre energy corresponds to a neutron wavelength $\lambda = 6.2712 \text{ \AA}$. The backscattered beam is then deflected from a (002) highly oriented pyrolytic graphite crystal into a neutron guide pointing to the sample table. The primary beam was chopped with a frequency of 48 Hz by a chopper with two apertures of 90° . The incident beam was limited to a size of $20 \times 20 \text{ mm}$ and the detector entrance window to $12 \times 12 \text{ mm}$. Transmission curves were measured with a counting time of 10 min.

2.2. *Time-resolved measurements of the transmitted beam*

For time-resolved experiments, a lithium glass detector in connection with a photomultiplier was used. The lithium glass contained 6.6 wt.% Li and was isotope enriched to 95% with ^6Li . The scintillation decay time of the detector system was 200 ns. Neutrons of 630.8 ms^{-1} velocity require $1.6 \mu\text{s}$ to pass the detection volume of the 1 mm-thick glass plate. This determines the best achievable time resolution for the experimental set-up. The detector signal was processed with conventional time-counting electronics and then fed into a computer-controlled multichannel analyser. The multichannel analyser time-channel width was set to $2 \mu\text{s}$ internal dwell time.

Three different types of experiments were performed. First, the time modulation of the transmitted neutron intensity was measured as a function of the vibration phase by synchronizing the acquisition electronics to the vibration frequency. The chopper wheel with two 90° apertures was run at 48 Hz. At this chopper frequency the neutron pulses have a duration of $\Delta t_p = 5.5 \text{ ms}$ and are long compared with the vibration period $T_p = 22.3 \mu\text{s}$. The transducer excitation voltage was 12 V. The incident beam was collimated to $20 \times 20 \text{ mm}$ and the detector entrance limited by a cadmium diaphragm to 6 mm diameter. Time spectra of the transmitted beam were acquired with a monochromatic incident neutron beam of energy width $\Delta E = \pm 0.35 \mu\text{eV}$, reflected from a stationary polished Si 111 monochromator, and with a polychromatic beam of energy width $\Delta E = \pm 7.4 \mu\text{eV}$, reflected with the monochromator Doppler drive operating at 6 Hz. Typical data-acquisition times were 1 h.

In the second experiment we recorded the time structure of transmitted neutron pulses which were long compared with the vibration period $\Delta t_p \gg T_p$. Now the

acquisition electronic was triggered to the chopper frequency set to the maximum value of 83 Hz. Increasing the frequency produced rectangular neutron pulses of $\Delta t_p = 3 \text{ ms}$ duration. The time response of the crystal to monochromatic neutron pulses of energy bandwidth $\Delta E = \pm 0.35 \mu\text{eV}$ was measured for three sample settings. First, the crystal was rotated by 3° out of the exact backscattering position and a time spectrum was recorded. This gave the pulse shape and duration of the incident neutron pulses affected only by absorption in the silicon sample. Then the crystal was aligned in the backscattering position and a time spectrum was recorded without exciting the sample into resonance vibrations. This experiment gave information about a possible influence of the nonvibrating crystal on the transmitted signal, e.g. if multiple-scattered and therefore delayed neutrons can also be observed with the nonvibrating perfect crystal. Finally, the resonance vibration was excited and the time structure of neutron pulses transmitted through the vibrating crystal set in backreflection was measured. Data acquisition continued until the same maximum count rates for all the three sample settings were reached. Data-acquisition times ranged from 3 h for the first experiment to 18 h when the vibrating sample was aligned in the backscattering position.

In the third experiment we measured the time response of the vibrating crystal to neutron pulses comparable in duration Δt_p with the vibration period T_p . Closing the 90° chopper apertures to slits of 2 mm width produced Gaussian-shaped neutron pulses of $\Delta t_p = 33 \mu\text{s}$ full width at half-maximum (FWHM). The same sequence of experiments as for neutron pulses of millisecond duration was then carried out, first with a monochromatic neutron beam of energy width $\Delta E = \pm 0.35 \mu\text{eV}$. Then the Doppler monochromator was operated at 1 Hz and the time structure of polychromatic pulses of energy width $\Delta E = \pm 1.23 \mu\text{eV}$ was recorded. Energies of incident neutrons then cover about half of the total scattering range of the vibrating crystal. Data-acquisition times ranged from 4 to 20 h.

3. Neutron transmission experiments on the backscattering spectrometer IN10

In this section we present results of time-resolved neutron transmission experiments through a vibrating $\lambda/2$ resonator. The studies are preceded by a time-integrated measurement of neutron transmission curves. This measurement confirms the previously predicted reflection shape and allows a comparison of the performance of a $\lambda/2$ resonator as a monochromator in backscattering geometry with crystals excited into higher harmonics.

3.1. Transmission curves

The transmission curve of the nonvibrating sample crystal has a FWHM of $\Delta E = 0.7 \mu\text{eV}$, which is the expected and previously measured resolution for a polished Si 111 monochromator/unpolished Si 111 analyser set-up on IN10 (Fig. 1). The curve recorded at 12 V transducer voltage is representative of the sample-excitation conditions maintained for all the time-resolved neutron transmission experiments. The shape of the transmitted intensity profile confirms previous calculations for a $\lambda/2$ resonator vibrating at 0.5 MHz (see Fig. 3 in Hock *et al.*, 1993). The particular shape of the diffraction profile of the $\lambda/2$ resonator is caused by a high neutron transmission in the outer regions of its scattering range and is a prerequisite for the time-resolved experiments. The full energy width of the diffraction profile at the baseline is $4.7 \mu\text{eV}$ and the FWHM equals $2.9 \mu\text{eV}$. After deconvolution with the instrumental resolution function, a vibration amplitude of $1.1 \mu\text{m}$ may be calculated from the corrected energy width of $2 \mu\text{eV}$. For this strain the sample transmission decreases to 7% in the reflection centre. The full line through the data points is the convolution of the calculated transmission profile (see Fig. 5) with the Lorentzian instrumental resolution function of FWHM $\Delta E = 0.7 \mu\text{eV}$ measured on the nonvibrating crystal.

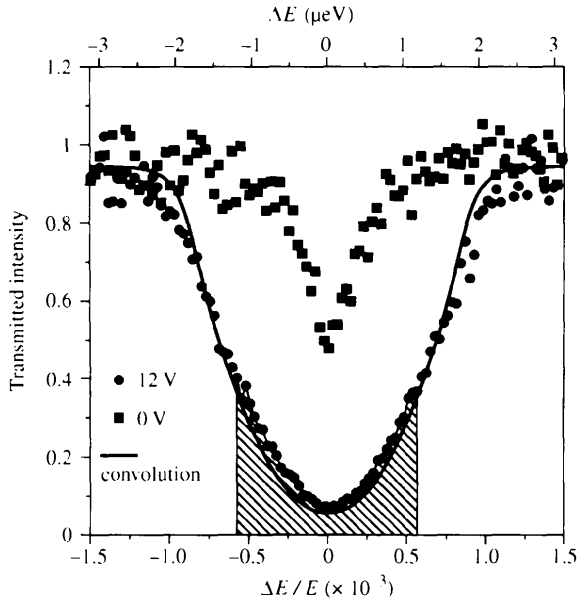


Fig. 1. Neutron transmission curves measured on the backscattering spectrometer IN10. The diffraction profiles are recorded with the nonvibrating crystal, excited in $\lambda/2$ resonance with a vibration amplitude of $1.1 \mu\text{m}$. The continuous line is the convolution of the simulated transmission profile (see Fig. 5) with a Lorentzian instrumental resolution function of FWHM $\Delta E = 0.7 \mu\text{eV}$. The hatched area indicates the energy width $\Delta E = \pm 1.23 \mu\text{eV}$ of the incident beam if the Doppler drive operates at 1 Hz.

The hatched area under the transmission curve indicates the energy width $\Delta E = \pm 1.23 \mu\text{eV}$ of the incident beam if the Doppler drive on IN10 operates at 1 Hz. This shows for a particular experiment (see Fig. 3a) the

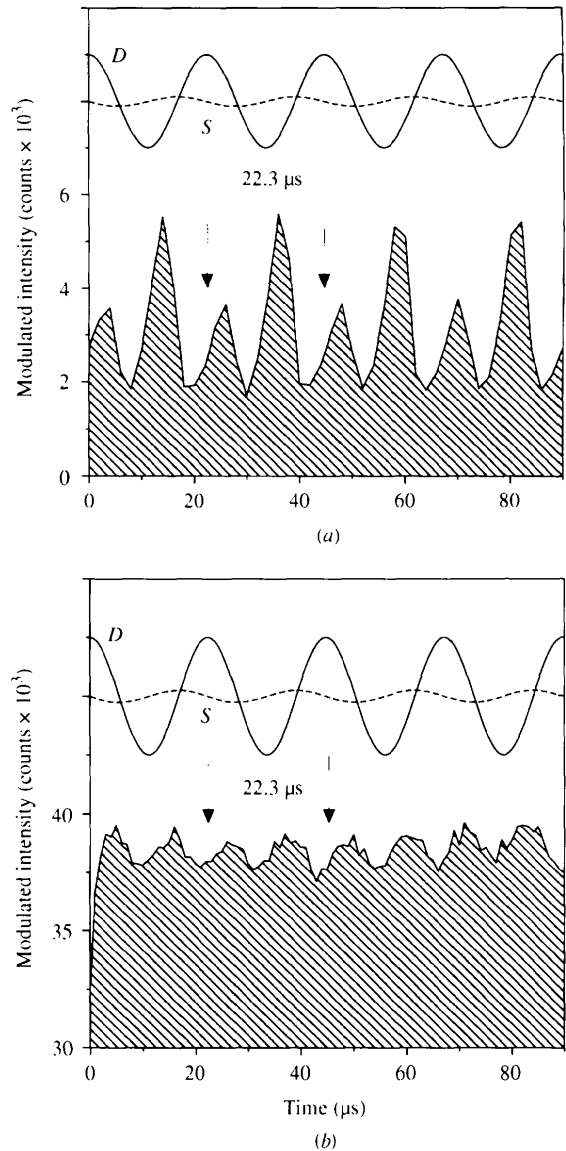


Fig. 2. The measured time modulation of a neutron beam transmitted through a silicon crystal vibrating in $\lambda/2$ resonance at 44.78 kHz. (a) Energy width of incident beam $\Delta E = \pm 0.35 \mu\text{eV}$ and (b) $\Delta E = \pm 2 \mu\text{eV}$. The quasimonochromatic beam of energy width $\Delta E = \pm 0.35 \mu\text{eV}$ is modulated with the vibration frequency $f_s = 44.78 \text{ kHz}$. The beam of energy width $\Delta E = \pm 2 \mu\text{eV}$ covering the total scattering range of the vibrating crystal is modulated with twice the vibration frequency $2f_s = 89.56 \text{ kHz}$. The modulation contrast decreases with increasing energy width of the incident beam. The solid (Doppler, *D*) and dashed (strain, *S*) lines schematically indicate the phase shift of the transmitted neutron pulses with respect to the Doppler and strain contributions to the total deformation field.

scattering range of the vibrating crystal compared with the energy width of the incident beam. Only neutrons within the hatched area contribute to the time structure of the transmitted signal.

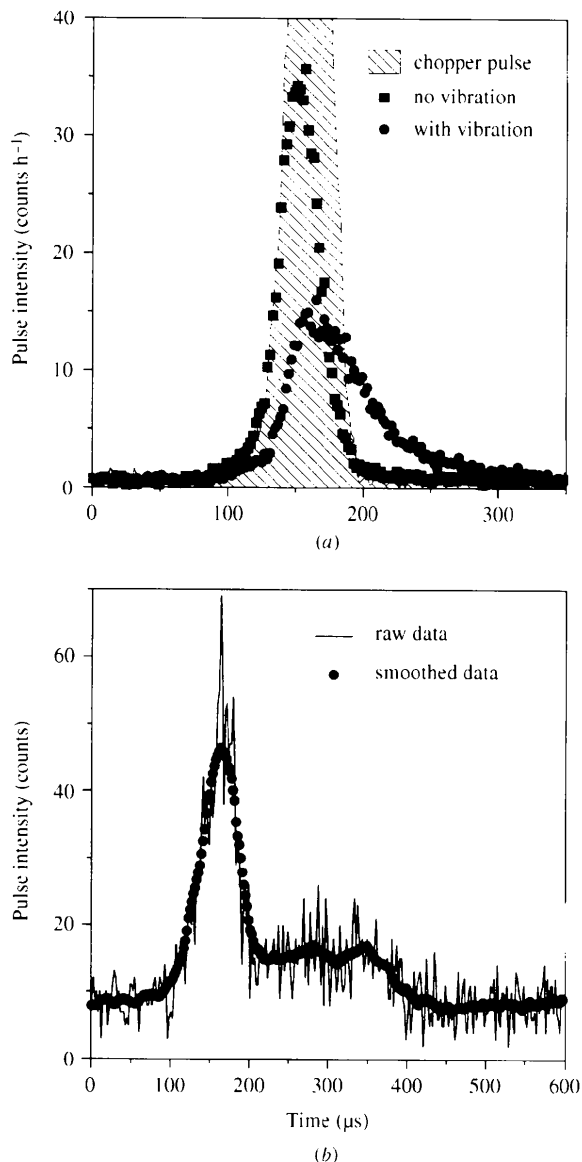


Fig. 3. The measured time structure of the transmitted beam for an incident pulse of duration comparable with the vibration period $\Delta t_p \simeq T_p$. (a) Neutron pulses of energy width $\Delta E = \pm 1.23 \mu\text{eV}$ were transmitted through the vibrating crystal in the backscattering position. Neutrons are stored in the resonator resulting in a $250 \mu\text{s}$ long decaying signal. (b) The time structure of the transmitted pulses changes significantly if the neutron beam is of smaller energy width $\Delta E = \pm 0.35 \mu\text{eV}$. After a directly transmitted signal, only neutrons with long transit times contribute to the time response of the vibrating crystal. As a guide to the eye, the raw data were smoothed with a Savitzky-Golay filter.

3.2. Modulation of the transmitted beam in response to a continuous incident beam

The transmitted beam was recorded as a function of the vibration phase. For an incident monochromatic beam of energy range $\Delta E = \pm 0.35 \mu\text{eV}$, the intensity is modulated with the vibration period $T_p = 22.3 \mu\text{s}$ (Fig. 2a). Diffraction peaks of different maximum intensity alternate and have modulation contrasts of 0.5 and 0.3, respectively. The intensity ratio of alternating maxima is $I_1/I_2 = 3/2$. The width of the modulation pulses at half height is $5 \mu\text{s}$. If the incident neutrons have energies which cover the full scattering range of the vibrating crystal, the modulation contrast decreases to 0.08 and the intensity of the non-time-dependent background increases (Fig. 2b). The modulation peaks now have equal intensity and the modulation frequency is twice the vibration frequency. In this measurement the Doppler monochromator oscillated at 6 Hz and the incident beam covered an energy range of $\pm 7.4 \mu\text{eV}$. This exceeds the scattering range of the crystal $\Delta E = \pm 2 \mu\text{eV}$ and the background therefore has an additional contribution from neutrons which were transmitted outside the scattering range.

3.3. Time structure of the transmitted beam in response to neutron pulses comparable in duration with the vibration period $\Delta t_p \simeq T_p$

The time structure of the transmitted beam was measured with incident neutron pulses comparable in duration with the vibration period $\Delta t_p \simeq T_p$. The shape of the chopper pulse was Gaussian with a FWHM of $33 \mu\text{s}$. The pulse transmitted through the nonvibrating crystal had a peak intensity of $90 \text{ neutrons h}^{-1}$ (Fig. 3a). Once the crystal was aligned to the backscattering position the pulse shape and FWHM remained unchanged, but the maximum pulse intensity dropped to $36 \text{ neutrons h}^{-1}$. Then the crystal was brought into resonance, the IN10 Doppler drive set to 1 Hz and the pulse time structure remeasured. Neutron energies now cover a range of $\Delta E = \pm 1.23 \mu\text{eV}$ and probe about half of the dynamic strain field $\Delta E = \pm 2 \mu\text{eV}$ of the vibrating crystal. A $250 \mu\text{s}$ -long decay of the transmitted signal shows neutrons released from the resonator after storage times equal to 11 vibration periods. Within the counting statistics, the observed intensity decay is a smooth function of time and no further structure is detected. Because the time structure should depend on the energy width of the incident neutron pulses, the experiment was repeated under identical vibration conditions with monochromatic pulses of width $\Delta E = \pm 0.35 \mu\text{eV}$. Now the transmitted signal shows a first pulse of $50 \mu\text{s}$ FWHM centred at the direct transit time, followed by a second broad intensity hump with an ill defined centre position at $300 \mu\text{s}$ (Fig. 3b). This second maximum detected $140 \mu\text{s}$ after the direct transit time is attributed to multiple-scattered neutrons. Because the

vibrating crystal reflects most of the neutrons back, the transmitted intensity is very low. Even in the first more intense pulse, the transmission is only 5 neutrons h^{-1} . Despite the weak signal, the time structure of the monochromatic transmitted beam is distinctly different from the smooth intensity decay in response to the polychromatic neutron beam.

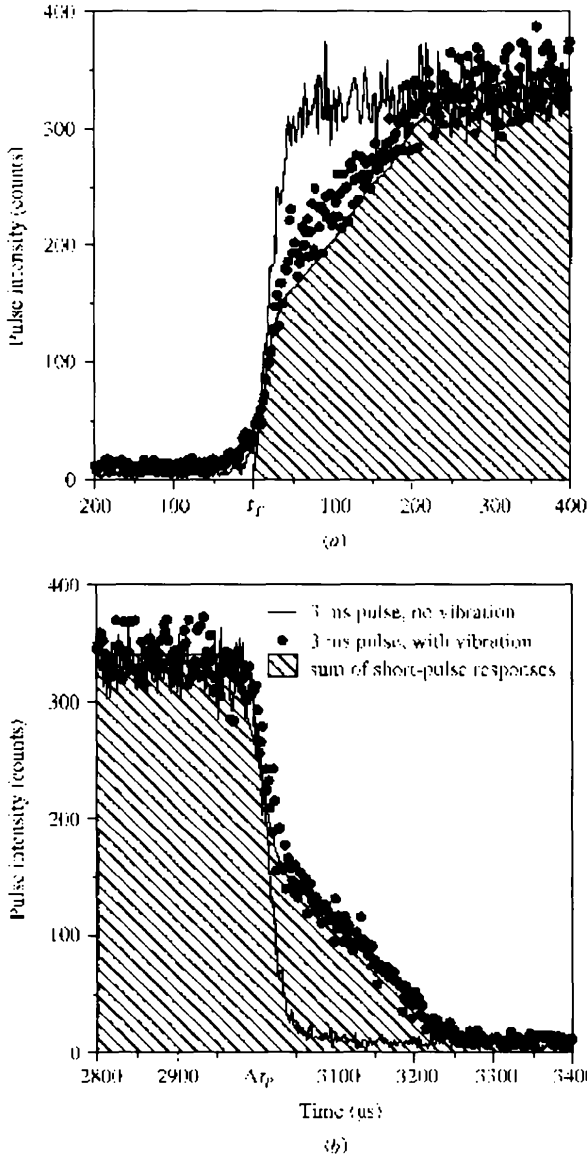


Fig. 4. The measured time structure of a transmitted neutron beam of energy width $\Delta E = \pm 0.35 \mu\text{eV}$. Incident neutron pulses are long compared with the vibration period $\Delta t_p \gg T_p$. Neutrons are stored in the vibrating crystal and (a) at the leading pulse edge the maximum transmitted intensity is reached about $250 \mu\text{s}$ later as measured on the nonvibrating crystal. (b) At the falling pulse edge a delayed signal of stored neutrons is observed for about $250 \mu\text{s}$.

3.4. Time structure of the transmitted beam in response to neutron pulses which are long compared with the vibration period $\Delta t_p \gg T_p$

Finally, the time response of the vibrating crystal to neutron pulses of $\Delta t_p = 3 \text{ ms}$ duration and energy width $\Delta E = \pm 0.35 \mu\text{eV}$ was recorded. Rectangular, symmetric neutron pulses with equally sharp rising and falling edges were transmitted through the silicon crystal. The pulse shape remained unchanged after the alignment of the sample in the backscattering position. Exciting the crystal into the resonance vibration then results in a skewed, asymmetric shape of the transmitted neutron pulses. The maximum neutron intensity at the leading pulse edge is reached about $250 \mu\text{s}$ later, as on the nonvibrating crystal (Fig. 4a). Accordingly, at the falling pulse edge, the neutron intensity decays over a time $T_D = 250 \mu\text{s}$ until it can no longer be significantly detected above the background signal (Fig. 4b). The experiment confirms that neutrons are stored in the dynamic Doppler-strain field. The hatched curves result from a summation of the measured short-pulse response shown in Fig. 3(b). The signal was summed in steps of $1 \mu\text{s}$ and reconstructs well the long-pulse response.

4. Results of Monte Carlo simulations

The backscattering and transmission of neutrons from a silicon-crystal bar vibrating in a $\lambda/2$ resonance in the kilohertz range were calculated with a program previously used to simulate the backscattering of neutrons from crystals vibrating in $n\lambda/2$ resonances at

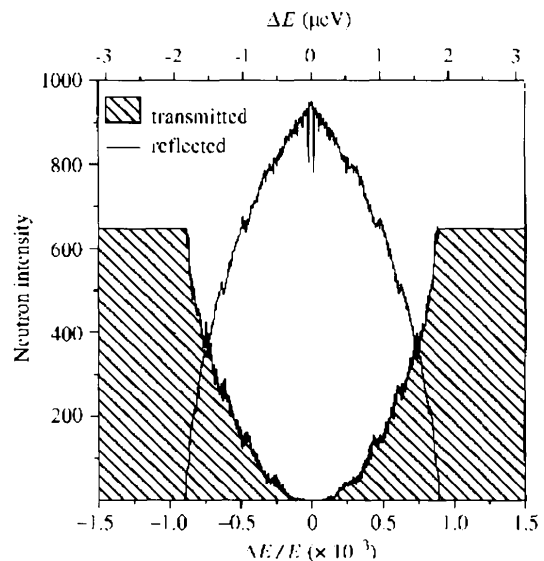


Fig. 5. Monte Carlo simulation of neutron transmission and reflection curves for a silicon crystal vibrating in $\lambda/2$ resonance at 44.78 kHz . The vibration amplitude is $1 \mu\text{m}$ and the scattering range of the crystal $\Delta E = \pm 1.9 \mu\text{eV}$.

megahertz frequencies. For the theory, simulation procedure and silicon-specific material parameters, readers are referred to Hock *et al.* (1993) and Hock & Kulda (1994). In the current simulations, the maximum energy range $\pm\Delta E/E$ scattered by the vibrating crystal was subdivided in 501 energy channels. The scattering histories of $N_N = 1000$ neutrons were simulated for each channel. The neutrons enter the crystal at vibration phases $\varphi = 2\pi/N_N$, such that the Doppler-strain field is probed on a dense grid of time intervals every one-

thousandth of the vibration period. The vibration amplitude chosen in the simulations was $u_0 = 1 \mu\text{m}$ which matches closely the sample strain excited in all time-resolved neutron transmission measurements on IN10. No Debye-Waller factor was taken into account in the calculations of the structure factor.

Some of the results, like the shape of the transmission curve and the time structure of the transmitted beam, can be compared directly with the experiments. Other information, such as the average number of reflections, or the average travelled path lengths and flight times for neutrons of energy E , is valuable for a further understanding and interpretation of the experimental results, even though this information is experimentally not accessible. At the end of this section we discuss the intensity distributions in the incident neutron beam for the various experimental settings on IN10. This information is used to explain differences between calculations and experimental results.

4.1. Transmission curves

Vibrating with an amplitude of $1 \mu\text{m}$, the $\lambda/2$ resonator reflects and transmits neutrons from an energy range $\Delta E = \pm 1.9 \mu\text{eV}$ (Fig. 5). That multiple scattering is frequent and will affect the transmitted as well as the reflected beam is already evident from the fine structure of the diffraction profiles. The ripples on the curves correspond to regions of slightly enhanced or reduced intensity compared with the average transmissivity or reflectivity. This structure depends only on the vibration frequency and is caused by multiple scattering. For some neutron energies close to the diffraction profile centre, even resonant neutron trapping occurs in the Doppler-strain field and leads to sharp intensity dips in the maximum of the backscattered reflection profile. This enhanced absorption occurs for neutrons which enter the crystal at vibration phases such that a long time-commensurate relation between the vibration period and the flight time between successive reflections is established. Since the local scattering probability is almost one in the weakly deformed crystal, all these neutrons are trapped until they are absorbed. In the centre of the scattered energy range, total reflection occurs and the sample transmission is zero. The sample transmission outside the scattering range is 67%, in accordance with a linear absorption coefficient of 0.04 cm^{-1} . Because the silicon crystal is absorbing, the backreflected neutron intensity does not reach the maximum reflectivity of one, equal to 1000 neutrons per energy channel used in the simulations. From the maximum reflectivity of 95% an absorption length of 1.4 cm is calculated for neutrons in the diffraction centre. This length is twice the mean free path of these single-scattered neutrons.

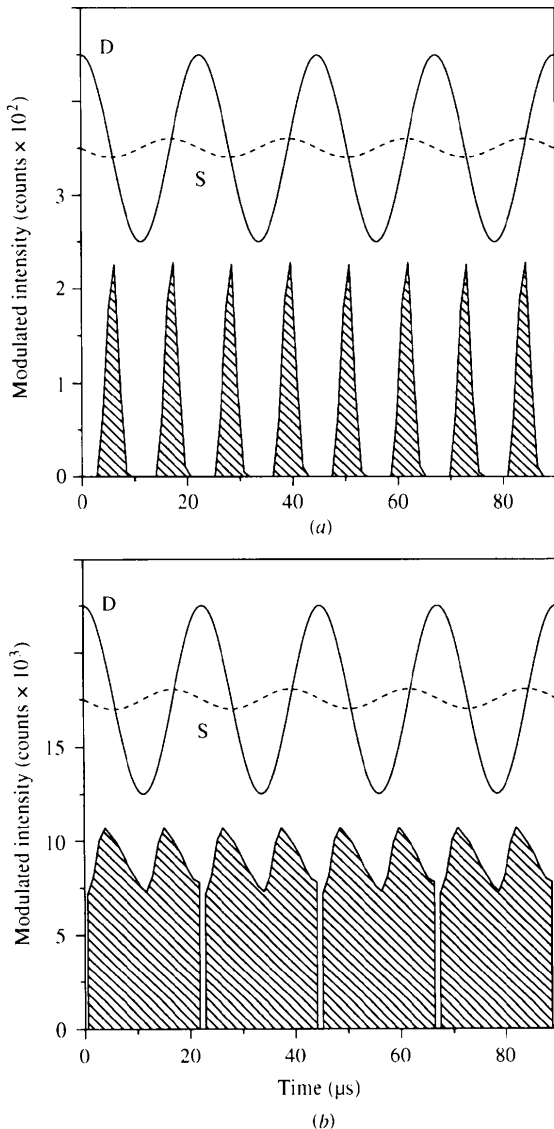


Fig. 6. The calculated time modulation of a neutron beam transmitted through a silicon crystal vibrating in $\lambda/2$ resonance at 44.78 kHz. The energy widths of incident beams are (a) $\Delta E = \pm 0.35 \mu\text{eV}$ and (b) $\Delta E = \pm 1.9 \mu\text{eV}$. The transmitted signals are modulated with twice the vibration frequency $2f_s = 89.56 \text{ kHz}$. The modulation contrast decreases with increasing energy width of the incident beam.

4.2. Modulation of the transmitted beam in response to a continuous incident beam

Neutrons were sorted according to the vibration phase at the moment they enter the crystal into phase channels of width $\Delta\varphi = 2\pi/20$. The channel width of $1.1 \mu\text{s}$ is comparable to the best time resolution of the scintillation detector used in the experiments. Calculations were carried out for incident neutron beams of energy widths $\Delta E = \pm 0.35 \mu\text{eV}$ (Fig. 6a) and $\Delta E = \pm 1.9 \mu\text{eV}$ (Fig. 6b). The energy width $\Delta E = \pm 0.35 \mu\text{eV}$ is comparable with the width of the diffraction profile measured on IN10 with the polished Si 111 monochromator/unpolished Si 111 analyser set-up. Neutrons from this energy range probe only the central part of the scattering range of the vibrating crystal. Pulses of equal intensity and $4.5 \mu\text{s}$ FWHM are transmitted. The pulse intensity is modulated with twice the vibration frequency and the modulation contrast is $(I_{\text{max}} - I_{\text{min}})/(I_{\text{max}} + I_{\text{min}}) = 1$. A neutron beam of energy width $\Delta E = \pm 1.9 \mu\text{eV}$ covers the total scattering range of the vibrating crystal. Again, the transmitted beam is modulated with twice the sound frequency but now has only a weak modulation contrast $(I_{\text{max}} - I_{\text{min}})/(I_{\text{max}} + I_{\text{min}}) = 0.2$ above a constant background of neutrons

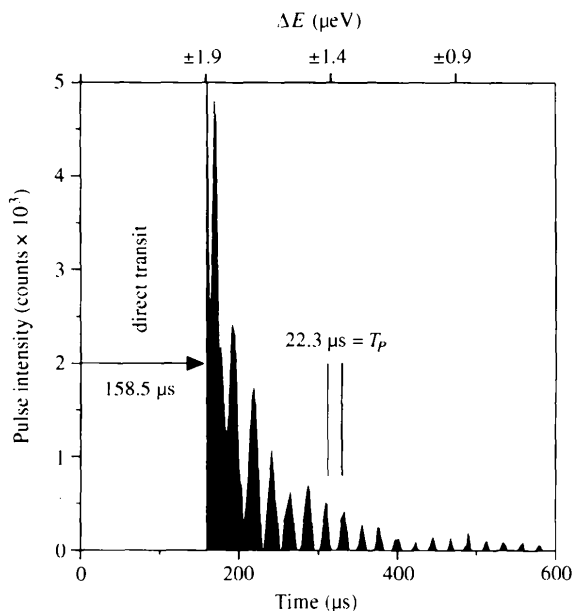


Fig. 7. The time structure of transmitted neutron pulses which are short compared with the vibration period $\Delta t_p \ll T_p$. Neutrons are released from the $\lambda/2$ resonator after multiples of the vibration period in a sequence of decaying pulses. The energy range $\Delta E = \pm 1.9 \mu\text{eV}$ of the incident neutron pulse covers exactly the scattering range of the vibrating crystal and the pulse sequence starts with directly transmitted neutrons at $158.5 \mu\text{s}$. 97% of the total transmitted signal has decayed after $250 \mu\text{s}$. The scale on the upper abscissa shows that the storage time of neutrons is correlated to their energy. Neutrons with energies close to the centre of the diffraction profile experience a higher number of reflections and therefore have longer storage times.

which contribute to the directly transmitted signal without phase relation to the vibration period of the crystal lattice.

4.3. Time structure of the transmitted beam in response to neutron pulses which are short compared with the vibration period $\Delta t_p \ll T_p$

Transmitted neutrons were sorted by their transit times in channels of $2 \mu\text{s}$ width. A pulse fulfilling the condition $\Delta t_p \ll T_p$ will be called a 'delta pulse'. For incident delta pulses, the simulated transmitted neutron signal in response to a beam of energy width $\Delta E = \pm 1.9 \mu\text{eV}$ is a sequence of pulses separated by the vibration period (Fig. 7). The pulse height decreases rapidly with increasing delay time. Of the total transmitted neutron intensity, 97% has decayed $250 \mu\text{s}$ after the direct transit time. The delay time at which neutrons contribute to the pulse sequence depends on their energy. Neutrons with energies close to the centre of the diffraction pattern at $2080 \mu\text{eV}$ all experience a high number of reflections, have long transit times and contribute only to the most delayed parts of the decaying transmitted signal. Neutrons with energies far from the centre energy are scattered in the maximum-amplitude regions of the Doppler-strain field, experience fewer reflections and accordingly have a short delay. They leave the resonator close to the direct transit time. Experiments with neutron beams of different energy widths should therefore result in transmitted signals with their maximum intensities at distinctly different delay times. The well separated pulses arriving at long delay times consist mostly of neutrons which experience an equal number of reflections. As an example, the neutrons within the pulse located at $275\text{--}300 \mu\text{s}$ were all reflected 20 times. The energy width of this specific pulse is $\Delta E = \pm 0.16 \mu\text{eV}$ and is only four times as broad as the width of the Darwin curve of the silicon 111 reflection $\Delta E = 0.08 \mu\text{eV}$. Neutrons contributing to the intensity maximum at the direct transit time passed the crystal without scattering, even though their energies are within the scattering range of the crystal. These neutrons enter the resonator at vibration phases such that they do not meet the Bragg condition.

4.4. Time structure of the transmitted beam in response to neutron pulses which are long compared with the vibration period $\Delta t_p \gg T_p$

Independently of the incident-pulse duration and shape, some of the neutrons are always stored by multiple scattering in the oscillating strain field and a decaying transmitted signal should also be observable on the falling edges of rectangular neutron pulses which are long compared with the vibration period. The time response of the vibrating crystal to long incident pulses of energy width $\Delta E = \pm 0.35$ and $\pm 1.9 \mu\text{eV}$ was simu-

lated by a quasicontinuous superposition of many delta-pulse time responses in steps of $1 \mu\text{s}$. On entering the vibrating crystal neutrons are stored and do not immediately contribute to the transmitted pulse. Therefore, the pulse rises more slowly to its maximum intensity compared with a pulse transmitted through the nonvibrating crystal (Fig. 8a). The 'mirror' image of this delayed-intensity rise on the leading edge of the transmitted pulses manifests at the falling pulse edge as a slow intensity decay (Fig. 8b). Calculated delayed

signals show a staircase-like intensity variation on both the rising and falling pulse edges. This structure arises as the consequence of the superposition of many delta-pulse responses and corresponds to an integration of pulse sequences as shown in Fig. 7. Observation of the staircase structure would be a strong indication of the existence of the predicted pulse sequence in response to the delta pulse. In Fig. 8(a) the time t_T is the transit time of the leading edge of a pulse with length $\Delta t_p = 3 \text{ ms}$. t_T is not the same for pulses of different energy width. Since the monochromatic pulse of energy width $\pm 0.35 \mu\text{eV}$ consists of neutrons which all have long

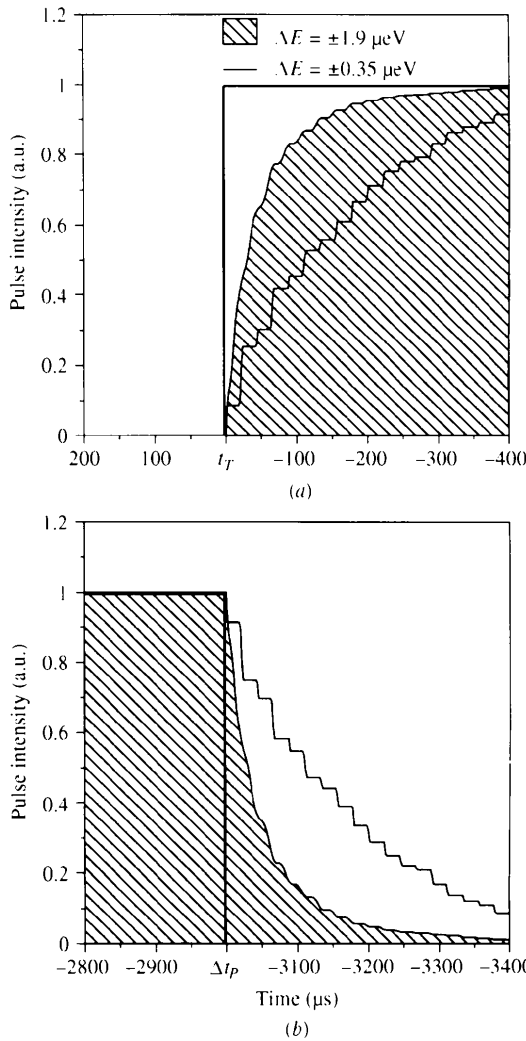


Fig. 8. The time structure of transmitted neutron beams of energy widths $\Delta E = \pm 0.35$ and $\pm 1.9 \mu\text{eV}$. Incident neutron pulses are long compared with the vibration period $\Delta t_p \gg T_p$. The neutron signals are calculated from a superposition of delta-pulse responses in steps of $1 \mu\text{s}$ and show a staircase structure. Neutrons are stored in the vibrating crystal and (a) at the leading pulse edge the maximum transmitted intensity is reached later compared with a pulse transmitted through the nonvibrating crystal. (b) At the falling pulse edge a delayed decaying signal of released neutrons is observed.

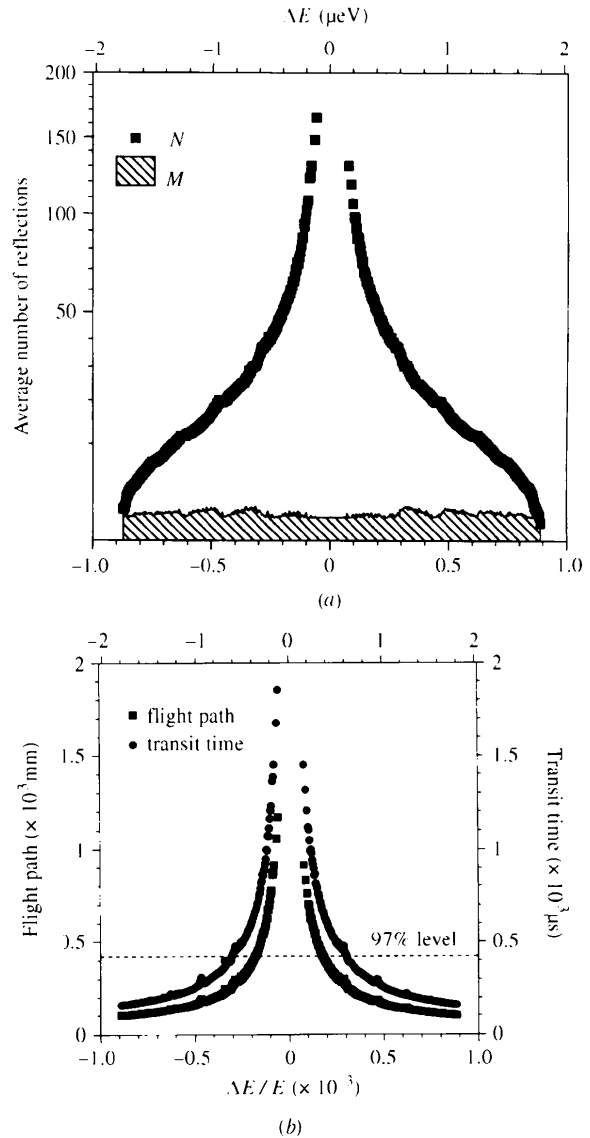


Fig. 9. (a) Average number of reflections experienced by transmitted (N) and backreflected (M) neutrons as a function of energy. (b) Average flight path and transit time of transmitted neutrons as a function of energy.

delay times (see Fig. 9b), this pulse would be more delayed than the $\pm 1.9 \mu\text{eV}$ pulse.

4.5. Energy dependence of multiple scattering

The average number N of reflections experienced by transmitted neutrons peaks towards the region of total reflection extending in energy from $-0.2 \leq \Delta E \leq 0.2 \mu\text{eV}$ (Fig. 9a). Neutrons with energies close to this region are reflected up to 165 times before they are finally transmitted. The average number M of reflections of backreflected neutrons is almost constant at 1 over the total scattering range of the dynamic gradient crystal. Rarely, neutrons are scattered three times or more before they are finally reflected back. The average flight paths and transit times of transmitted neutrons depend directly on the number of reflections. Both quantities increase rapidly towards the energy region of total reflection (Fig. 9b). The flight path may be as long as 1.2 m corresponding to a transit time of 1.9 ms. These extreme scattering histories are rare and the vast majority of neutrons have a much shorter flight path and transit time. 97% of neutrons leave the crystal in a time interval of 250 μs after direct transit and 99% of the stored neutrons are released after 400 μs .

4.6. The intensity distribution in the incident energy spectra

Since the contribution of neutrons to the time structure of the transmitted beam is dependent on their energy, the intensity distribution of the incident beam will have an influence on the transmitted signal. Knowledge of the incident-beam spectrum is therefore important for interpreting differences between calculations and experiments. The Monte Carlo simulations are based on a constant neutron intensity over the whole range of energies. An identical number of neutrons per energy channel are used in the calculations. The true neutron flux for the various experimental situations on IN10 is not constant over the incident neutron spectrum. Three types of neutron spectra occurred in this work. The energy width of the neutron beam reflected from a perfect silicon 111 monochromator mounted on the Doppler drive of IN10 increases proportionally with the Doppler frequency f_D e.g. $\Delta E/E (\mu\text{eV}) = \pm 1.23 f_D (\text{Hz})$. The neutron flux in this energy range is given by an inverse sinus function multiplied by the reflectivity profile of the graphite deflector and by the transmission characteristics of the neutron guides. The incident-beam intensity is approximately constant over two-thirds of the total reflected energy range. If the scattering range of the vibrating crystal is smaller than or equal to the width of this intensity plateau, the assumption of a constant neutron flux is justified. Once the scattering range of the vibrating crystal becomes broader than the maximum energy range reflected from the Doppler

monochromator, the nonuniform intensity distribution in the incident beam becomes apparent in the experiment. The neutron flux is then enhanced for energies in the outer regions of the diffraction profile away from the centre energy 2080 μeV . Using a stationary silicon monochromator, the intensity distribution of the neutron spectrum at the sample position is given by the convolution of the Darwin curve of the silicon 111 reflection with the nonideal reflection characteristics of the neutron guide and the pyrolytic graphite deflector. A Lorentzian intensity distribution with an energy width of $\Delta E = \pm 0.35 \mu\text{eV}$ results if the beam is analysed with an unpolished silicon crystal.

5. Discussion

In this section the agreement and points of disagreement between the experimental results and the calculations are discussed. Some difficulties encountered in the time-resolved experiments are reported.

5.1. Transmission curves

If the calculated transmission curve is convoluted with the experimental resolution function, experimental and calculated neutron transmission profiles are in good agreement. The measurement confirms the predicted shape of the diffraction profile for transmission through a $\lambda/2$ resonator (Hock & Kulda, 1994). In contrast to the measurements on crystals excited to higher harmonics $n\lambda/2$ ($n \geq 5$) (Hock *et al.*, 1993), the neutron transmission curves are not box shaped. A considerable neutron flux is transmitted in the outer regions of the scattering range. Because of this smaller integrated reflectivity, $\lambda/2$ resonators perform less well as monochromators in backscattering geometry than crystals excited to higher harmonics. At identical strain the shape of the transmitted profile depends only on the mode of vibration and not on the excitation frequency. A $\lambda/2$ resonator vibrating at some 10 kHz will transmit the same profile shape as a $\lambda/2$ resonator vibrating at megahertz frequencies. On the other hand, it is this higher transmissivity of the $\lambda/2$ resonator that makes it attractive for measurements of the time structure of neutron beams transmitted through an oscillating Doppler-strain field.

5.2. Modulation of the transmitted beam in response to a continuous incident beam

Monte Carlo simulations predict a modulation of the transmitted beam with twice the vibration frequency and a modulation contrast that decreases with increasing energy width of the incident neutron beam. This modulation frequency was observed for the incident beam of energy width $\Delta E = \pm 1.9 \mu\text{eV}$. The dependence of the modulation contrast on the energy width of the neutron beam was confirmed. The modu-

lation contrast increases with decreasing energy width of the incident neutron beam. A difference between calculations and experiment is evident for the modulation of the monochromatic beam. Successive pulses have different intensities and therefore the transmitted beam is modulated with the vibration frequency itself. Such a modulation frequency should not occur for a harmonically oscillating non- or weakly absorbing crystal. The two pulses transmitted within a vibration period correspond to the contraction and dilatation phases of the resonator. A difference in the pulse heights must be attributed to a different transmissivity of the crystal during contraction and dilatation. This effect is known from neutron diffraction experiments on strongly absorbing vibrating crystals of InSb (Mikula *et al.*, 1992). The asymmetry in reflectivity every half-cycle of the vibration is caused by a sound-induced additional attenuation coefficient which depends on the direction of the deformation gradient with respect to the scattering vector. Because of multiple scattering, the quasimonochromatic neutrons contributing to the modulated beam in our experiment all have flight paths longer than 0.5 m reaching up to more than 1 m. Then μt ranges from $2 \leq \mu t \leq 4$ even for the weakly absorbing silicon crystal and the experimental situation becomes comparable to the diffraction experiments on InSb. An attenuation coefficient dependent on the direction of the deformation gradient with respect to the scattering vector is a dynamical effect we do not take into account in the Monte Carlo simulations.

5.3. Time structure of the transmitted beam in response to neutron pulses which are short or comparable with the vibration period $\Delta t_p \leq T_p$

The measured pulse decay time of 250 μs is in good agreement with the results of Monte Carlo simulations. Since no neutron pulses shorter than 33 μs FWHM could be generated with sufficient intensity, the experimental pulse width was longer than the vibration period of 22.3 μs and the convolution of the expected pulse sequence with the Gaussian chopper pulse resulted in the observed continuous decay. In principle, neutron pulses of about 1 μs length which is sufficiently short for a measurement of the predicted time structure can be generated. Since the short pulses carry a low neutron flux, the feasibility of the experiment is then a question of data-acquisition time. There are two reasons for the fast intensity decay of the transmitted neutron signal. Pulses released from the resonator after long storage times are affected the most by absorption. These pulses correspond to neutrons with the longest flight paths in the crystal. The second reason is the transmission characteristic of the $\lambda/2$ resonator. Towards the central part of the diffraction curve the transmission decreases to zero. The closer the neutron energy gets to the region of total reflection, the longer

is the potential storage time of the particles, but the smaller is the probability of being transmitted. Most of the neutrons with potentially high numbers of reflections and long storage times are reflected back. Both effects contribute to the decay of the transmitted pulse sequence.

The delay time of neutrons depends on their energy with respect to the scattering range of the crystal. A first indication of this dependence was seen in the experiment. If the energy width of the neutron beam covers the total scattering range of the vibrating crystal, a smoothly decaying pulse is transmitted with a single maximum at the direct transit time. A primary neutron beam of narrow energy width results in two intensity maxima, the first located at the direct transit time and a second broad intensity maximum delayed by 140 μs . The first pulse is due to directly transmitted neutrons and neutrons with short delay times. The weaker second maximum is formed by stored neutrons with long delay times as is expected from the energy width of the incident beam. That the time structure of the transmitted beam must depend on the energy distribution of the incident neutrons is understood by the average number of reflections as a function of energy. Neutrons with energies close to the centre of the diffraction curve experience the most reflections and have the longest storage times. They only contribute to the most delayed parts of the transmitted signal. The opposite argument holds for neutrons with energies far from the centre energy. The vibrating $\lambda/2$ resonator thus will generate a transmitted beam in which the neutrons are sorted in time and by their energy. Further, the calculations show that the vibrating crystal potentially transforms a short single pulse into a sequence of pulses with an energy width about one order of magnitude smaller than the energy width of the original incident pulse.

The monochromatic-beam short-pulse experiment naturally results in a weak transmitted signal. The incident flux is low and most of the neutrons are reflected back. The experiments are based on only a few percent of the incident neutron flux. To observe neutrons with the longest storage times, the Lorentzian intensity distribution of the primary beam is unsuitable. The incident flux peaks in the region of total reflectivity and only neutrons from the tails of the Lorentzian distribution have a considerable transmission probability. We can imagine two modifications of the experiment to overcome this experimental difficulty. Both are based on a shift of the narrow incident energy distribution away from the region of total reflection. To shift the energy distribution across the scattering range of the vibrating crystal one could use a CaF_2 thermal-gradient monochromator, or as in the experiments of Schuster *et al.* (1991) and Jericha *et al.* (1996) apply a magnetic field. With both methods, the Doppler-strain field could be probed step by step with a resolution determined by the energy width of the incident beam.

5.4. *Time structure of the transmitted beam in response to neutron pulses which are long compared with the vibration period $\Delta t_p \gg T_p$*

The experiments on IN10 with neutron pulses of 3 ms duration confirm the calculations. The predicted pulse-shape asymmetry caused by stored neutrons was observed. The decay time for the stored neutron signal of 250 μs is in good agreement with the simulations. The observed decay is located between the curves for a polychromatic beam of width $\Delta E = \pm 1.9 \mu\text{eV}$ and a beam of energy width $\Delta E = \pm 0.35 \mu\text{eV}$. This intermediate decay is due to a contribution of directly transmitted neutrons to the time response. A superposition of many measured short-pulse responses models exactly the decaying intensity response to neutron pulses of millisecond duration. The staircase structure which should be superimposed on the delayed parts of the transmitted pulses was not observed. If present, this structure is hidden in the counting statistics. Since experiments with long neutron pulses do not suffer as much from low neutron flux as experiments with pulses of microsecond duration, the staircase structure may be easier to measure. To gain neutron flux in future experiments, the chopper pulse sequence could be modified to supply pulses of 300 μs length with a duty cycle of 1:1. Because 98% of the transmitted signal has decayed after this time, no observable frame overlap will occur. A further gain in transmitted intensity can be achieved by experimenting with larger vibration amplitudes and by matching the energy width of the incident beam exactly to this enhanced scattering range.

6. Conclusions

The basic prediction of the Monte Carlo simulation was confirmed by experiments on the backscattering spectrometer IN10. Neutrons are stored in the oscillating Doppler-strain field of the $\lambda/2$ resonator by multiple reflections. About 97% of the stored neutrons leave the crystal within 11 vibration periods, equal to a maximum delay of 250 μs after the direct transit time. In future experiments it may be possible to obtain precise results on the energy dependence of the time structure of transmitted pulses. The complete scattering range of the

vibrating crystal could be successively probed with an incident neutron beam of small energy width, which is shifted over the scattering range of the crystal. This may be possible using a thermal-gradient crystal as monochromator, or by shifting the energy of incident neutrons reflected from a perfect silicon monochromator by a magnetic field.

We thank A. Oed, B. Frick and A. Snigirev for the loan of electronic equipment indispensable for the time-resolved measurements. Special thanks to P. Joubert-Bousson who provided technical support on IN10.

References

- Buras, B., Giebultowicz, T., Minor, W. & Rajca, A. (1972). *Phys. Status Solidi A*, **9**, 423–433.
- Hock, R. & Kulda, J. (1994). *Nucl. Instrum. Methods A*, **338**, 38–43.
- Hock, R., Vogt, T., Kulda, J., Mursic, Z., Fuess, H. & Magerl, A. (1993). *Z. Phys. B Condens. Matter*, **90**, 143–153.
- Iolin, E. M., Rusevich, L. L., Vrana, M., Mikula, P. & Lukas, P. (1996). *Phys. Status Solidi B*, **195**, 21–35.
- Jericha, E., Carlile, C. J. & Rauch, H. (1996). *Nucl. Instrum. Methods A*, **379**, 330–334.
- Kulda, J., Mikula, P., Vrana, M., Michalec, R. T. & Vavra, J. (1981). *Nucl. Instrum. Methods*, **180**, 89–92.
- Kulda, J., Vrana, M. & Mikula, P. (1988). *Physica B*, **151**, 122–129.
- Michalec, R., Mikula, P., Vrana, M., Kulda, J., Chalupa, B. & Sedlakova, L. (1988). *Physica B*, **151**, 113–121.
- Michalec, R., Sedlakova, L., Chalupa, B., Galociova, D. & Petrzilka, V. (1971). *Acta Cryst. A* **27**, 410–414.
- Mikula, P., Kulda, J., Vrana, M. & Michalec, R. T. (1980). *Phys. Status Solidi A*, **61**, K67–K69.
- Mikula, P., Lukas, P. & Kulda, J. (1992). *Acta Cryst. A* **48**, 72–73.
- Mikula, P., Michalec, R., Cech, J., Chalupa, B., Sedlakova, L. & Petrzilka, V. (1974). *Acta Cryst. A* **30**, 560–564.
- Mikula, P., Michalec, R. T. & Vavra, J. (1976). *Nucl. Instrum. Methods*, **137**, 23–27.
- Schuster, M., Carlile, C. J. & Rauch, H. (1991). *Z. Phys. B Condens. Matter*, **85**, 49–57.
- Schuster, M., Rauch, H., Seidl, E., Jericha, E. & Carlile, C. J. (1990). *Phys. Lett. A* **144**, 297–300.
- Stoica, A. D. & Popovici, M. (1984). *J. Appl. Cryst.* **17**, 315–319.